and to have no prominent effect on the fine structure. It does not reveal itself by splitting a degeneracy, as in the case of the hydrogen atom. Our calculations of the fine structure and its radiative corrections will be published in detail later.

We wish to thank Professor A. S. Wightman for valuable guidance and help in this problem, and the Atomic Energy Commission for support through a Predoctoral Fellowship.

* The work outlined here is part of a Ph.D. thesis to be submitted to Princeton University.

† This work was supported in part by the AEC.

[1] R. H. Dicke and T. A. Pond (private communication).

[2] M. Deutsch (private communication).

[3] J. Pirenne, Arch. sci. phys. et nat. **28**, 233 (1946); **29**, 121, 207, and 265 (1947). Pirenne omits a term $\pi e^2\hbar^2\delta(r)/m^2c^2$ from the orbital interaction, and his spin-orbit energy should be multiplied by 3/2.

[4] V. B. Berestetski, J. Exptl. Theoret. Phys. (U.S.S.R.) **19**, 1130 (1949). See also V. B. Berestetski and L. D. Landau, J. Exptl. Theoret. Phys. (U.S.S.R.) **19**, 673 (1949). Berestetski's expressions for the interactions are correct. His evaluation of $\overline{V}_4$, however, seems to be in error for $l \neq 0$, for it is too large by a factor of two.

Ionization Potentials and Probabilities Using a Mass Spectrometer

R. E. Fox, W. M. Hickam, T. Kjeldaas, Jr., and D. J. Grove
Westinghouse Research Laboratories, East Pittsburgh, Pennsylvania
(Received October 4, 1951)

A METHOD for determining ionization potentials and ionization probability curves has been devised which eliminates the difficulties arising from uncertainties in the energy of the bombarding electrons.[1]

A sketch of the ion source is shown in Fig. 1(a). Electrons leaving the filament are accelerated into the ionization enclosure by the potential V_1. The intermediate electrode 4 is maintained at a negative potential V_R with respect to the filament so as to prevent the low energy electrons in the distribution from entering the ionization chamber. The increase in the ion current observed when the absolute value of V_R is decreased by ΔV_R, keeping V_1 fixed, represents the ion current produced by a beam of electrons monoenergetic within ΔV_R. If V_{4M} is the larger, and V_{4m} the smaller in absolute value of the two corresponding V_4 readings, this then uniquely determines the maximum and minimum energy of the electrons producing the observed difference in ion current [see Fig. 1(b)]. If now the ion current difference is measured and plotted as a function of V_{4M}, keeping V_R constant, this difference will go to zero at the ionization potential. This curve represents the ionization probability as measured with an electron beam monoenergetic within ΔV_R. In a case where the ionization probability varies linearly with the electron energy, for values of V_{4M} greater than ΔV_R plus the ionization potential, the observed curve should be linear. For values of V_{4M} within ΔV_R above the ionization potential the curve is essentially parabolic, approaching the axis with zero slope at the ionization potential. In the measurements described here, ΔV_R was 0.1 volt and usually no points were taken for V_{4M} within this region. This amounts to extrapolating over the small interval ΔV_R. It may be proved that this will yield a value for the ionization potential too high by $\Delta V_R/2$. To compensate for this, the experimental curves were plotted as a function of the average value of V_4 instead of V_{4M}.

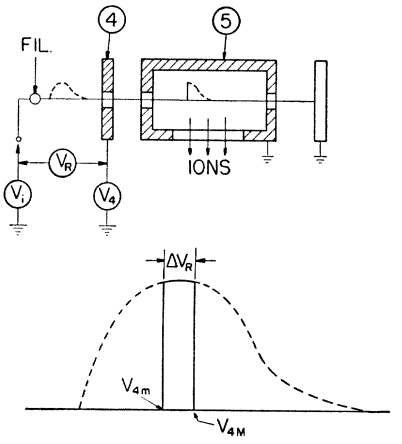

FIG. 1. (a) A sketch of the ion source showing the electrode structure and the voltage references. (b) A distribution in electron energy which is modified by the retarding potential to give the equivalent of a monoenergetic electron beam.

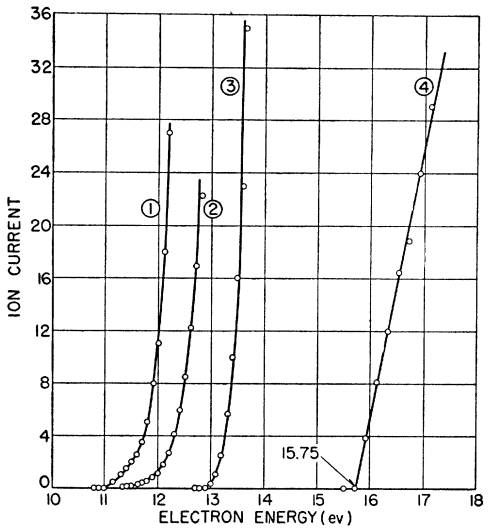

FIG. 2. Ionization probability curves for argon 40^+. Run (1) taken by conventional method. Run (2) taken by conventional method with 0.1 sensitivity at the amplifier. Run (3) the ion difference curve using a retarding potential on the electrons, but with an ion-draw-out voltage of 3 volts. Run (4) the ion difference curve obtained using both a retardation of the electrons and pulsed fields on ions and electrons.

Since the energy scale is determined by the potential between the retarding electrode 4 and the ionization chamber 5 [see Fig. 1(a)] the effect of the contact potentials between the filament and the accelersting electrodes is eliminated. Those contact potentials which can arise between the accelerating electrodes have been reduced or eliminated by gold plating all surfaces.

To obtain ion currents of sufficient magnitude, it is necessary to apply a small electric field across the ionization chamber in a direction normal to the electron beam. In past experiments, this ion-draw-out field created an inhomogeneity and uncertainty in the electron energy. In the present experiments this difficulty has been overcome by giving the electron current and the ion-draw-out voltage a pulsed time dependence such that the electrons reach the ionization chamber only when the draw-out field is zero.

Because magnetic collimation of the electron beam is employed, one might expect that the transverse (spiralling) velocity of the electrons would give rise to a considerable spread in electron energy, which would lead to "tailing" of the ionization probability curve in the region of onset. Experimentally, this "tailing" is not observed, indicating that some mechanism serves to prevent electrons with appreciable transverse energy from reaching the ionization chamber.

Since the electrons are moving very slowly near the retarding plate, space charge effects are quite important in this experiment. By measuring the apparent ionization potential as a function of the electron current, and extrapolating to zero current, a correction term was obtained which was of the order of 0.2 volt for the work reported here. Modifications are underway which should reduce this effect.

Preliminary measurements have been taken on argon (40^+), krypton (84^+), nitrogen (28^+), and carbon monoxide (28^+). In all

cases, the measured ionization potentials agree with the spectroscopic values within 0.1 volt, and the ionization probability curves obtained were straight lines for energies less than 2 ev above the ionization potentials. Figure 2 gives a comparison of the ionization probability curve for argon obtained by this method with that obtained by the conventional method. Runs 1 and 2 show a typical curve under the influence of thermal energy spread in the electrons, contact potentials, and the ion-draw-out field. Run 3 shows a curve in which the thermal energy spread has been narrowed to within 0.1 ev and the contact potential between the filament and the electrodes has been eliminated. The slight "tailing" in curve 3 is attributed to the inhomogeneity in electron energy introduced by the ion-draw-out field. In run 4 all these effects have been eliminated, yielding a straight-line ionization probability curve going to zero at a value which agrees closely with the spectroscopic value of the ionization potential.

In conclusion, the authors wish to express their appreciation to Dr. T. Holstein for his contributions to the method described.

[1] See, for example, J. J. Mitchell and F. F. Coleman, J. Chem. Phys. 17, 44–55 (1949).

Nuclear Structure in Fission

L. E. Glendenin, E. P. Steinberg, M. G. Inghram, and D. C. Hess
Argonne National Laboratory, Chicago, Illinois
(Received September 10, 1951)

MASS spectrometric investigations of the relative abundances of fission product species from uranium fission have been made by Thode and co-workers[1] and Inghram and co-workers.[2] This type of measurement is capable of high precision and, with appropriate normalization, permits the establishment of fission yields to a much higher degree of accuracy than the present radiochemical techniques.

The early results of Thode *et al.* on Kr and Xe abundances in fission indicated abnormally high yields at masses 133 and 134 and, perhaps, in the region 83–86 as well. One would, of course, expect some fine structure in the yield-mass curve as a result of known delayed neutron effects, but these, at most, are of the order of ~0.5 percent in fission yield and cannot account for the magnitude of Thode's results. Recent radiochemical studies on Te and I fission yields have also indicated a high yield at mass 134.[3]

A proposal to account for the observed anomalies which was made by one of us,[4] based on the boiling-off of an extra neutron from the fission fragments containing 51 or 83 neutrons, appeared to be qualitatively successful. This hypothesis, however, predicts a low yield at mass 137 which has been shown not to be the case.[5] The discrepancy between observation and prediction here led Thode to propose a possible preference for an 82-neutron configuration in the fission act in addition to a neutron boil-off effect following fission. It should be noted that an extension of the neutron boil-off hypothesis to fission fragments containing three and five neutrons in excess of a closed shell would account for the observed "normal" yield of mass 137. Fission yield determinations of masses complementary to the mass region 133–137 should establish whether the fine structure observed is the result of a preferential mode of fission or of phenomena following fission. Such studies are now in progress at this laboratory.

In the present work some interesting effects have been noted in the isotopic abundances of Mo and Zr produced in the fission of uranium. These data, together with normalized data on fission Xe and Kr (Thode) and Nd (Inghram), are presented in Fig. 1 where they are compared with the smooth radiochemical fission yield-mass curve.

Since the results obtained from these investigations are relative abundances, the data of one element must be fitted to those of another in some, as yet arbitrary, manner. For the present we have normalized the Xe data to the radiochemical yield-mass curve at mass 131 (=2.8 percent). Since the ratio of total Xe to Kr was

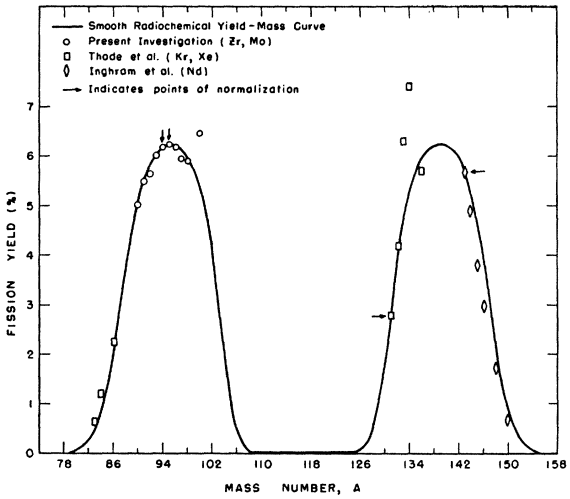

FIG. 1. Comparison of smooth radiochemical U^{235} fission yield data with mass spectrometric data.

obtained in Thode's work, this also fixes the Kr yields. Likewise, the Nd data were normalized to the radiochemical curve at mass 143 (=5.7 percent), Zr was normalized at mass 94=6.20 percent and Mo at 95=6.25 percent. Experiments are in progress to establish absolute abundances of Zr, Mo, and Ru in fission and thus obviate some of the difficulties of normalizing the relative abundance data.

It should be noted, however, that whatever normalization is employed, the present data for Mo indicate an abnormally high yield in the mass region 98–100. The anomalies in the mass 133–136 region are also quite evident on this linear plot. The original Kr^{86} and Xe^{136} data have been corrected for known delayed neutron emission. Thus, the data are corrected for the significant changes known to take place after fission. If a value of 2.5 for the number of neutrons per fission is taken for U^{235}, the data may be plotted as in Fig. 2, with the heavy group reflected over the light group such that the masses of complementary fission products sum to 233.5. In such a "folded" curve the coincidence of the anomalies at masses 98–100 *vs* 133–136 becomes obvious. Although neutron boil-off effects may be operating in the 133–137 mass region (the region in which 82 neutrons are present), there does not appear to be any reasonable basis for this effect in the region of mass 100. The high yield at Mo^{100}, then, suggests a preference for this mass in the fission act, perhaps as the complement of a preferred 82-neutron shell in the heavy fragment.

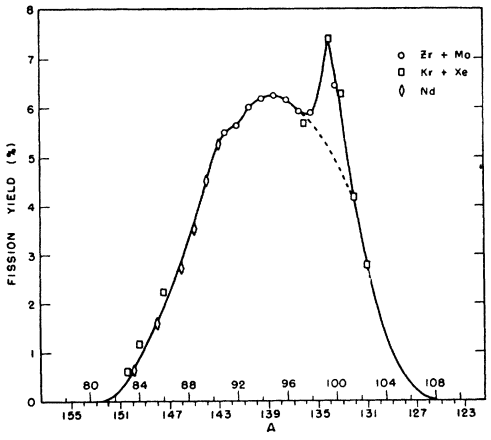

FIG. 2. Mass spectrometric yield-mass curve in U^{235} fission.